International Journal of Biochemistry and Cell Biology 110 (2019) 111–121

Contents lists available at ScienceDirect

International Journal of Biochemistry and Cell Biology

journal homepage: www.elsevier.com/locate/biocel

Glutamate affects the CYP1B1- and CYP2U1-mediated hydroxylation of arachidonic acid metabolism via astrocytic mGlu5 receptor

Xuming Yu[a,1], Juan Wu[a,1], Mingbai Hu[b,1], Jinhua Wu[a], Quanfei Zhu[c], Zheqiong Yang[a], Xianfei Xie[a], Yu-Qi Feng[c], Jiang Yue[a,d,*]

[a] Department of Pharmacology, Wuhan University School of Basic Medical Sciences, Wuhan, 430071, China
[b] Department of Oncology, Zhongnan Hospital of Wuhan University, Hubei Key Laboratory of Tumor Biological Behaviors & Hubei CancerClinical Study Center, Wuhan, 430071, China
[c] Key Laboratory of Analytical Chemistry for Biology and Medicine (Ministry of Education), Department of Chemistry, Wuhan University, Wuhan, 430071, China
[d] Hubei Province Key Laboratory of Allergy and Immunology, Wuhan, 430060, China

ARTICLE INFO

Keywords:
Cytochrome P450
Brain
Hydroxyicosatetraenoic acid
Glutamate

ABSTRACT

The extrahepatic CYP enzymes, CYP1B1 and CYP2U1, have been predominantly found in both astrocytes and brain microvessels. We investigated the alteration in the production of hydroxyeicosatetraenoic acids (HETEs) from arachidonic acid (AA) mainly via CYP1B1 and CYP2U1 by glutamate. CYP1B1 and CYP2U1 mRNA levels were dose-dependently induced by glutamate in human U251 glioma cells and hCMEC/D3 blood-brain barrier cells. The increases in the CYP1B1 and CYP2U1 mRNA levels and the binding of CREB to *CYP1B1* and *CYP2U1* promoters following glutamate treatment were attenuated by mGlu5 receptor antagonist. The mRNA levels of CYP1B1 and CYP2U1 were increased in the cortex, hippocampus, and cerebellum from adult rats that received a subcutaneous injection of monosodium L-glutamate at 1, 3, 5, and 7 days of age; meanwhile, the protein levels of CYP1B1 and CYP2U1 in the astrocytes were induced by glutamate. Glutamate treatment significantly increased the production of 5-HETE, 8-HETE, 11-HETE, and 20-HETE in the cortex and cerebellum. These data suggested that the neuron-astrocyte reciprocal signaling can change the CYP-mediated AA metabolism (e.g. EETs and HETEs) in astrocytes via its specific receptor.

1. Introduction

Astrocytes have historically thought to be passive housekeeping cells. Brain astrocytes in primary culture have been shown to metabolize membrane phospholipids to produce arachidonic acid (AA) (Stella et al., 1994a), which can be used to synthesize vasodilatory substances such as prostaglandins and epoxyeicosatrienoic acids (EETs) within astrocytes (Amruthesh et al., 1993; Alkayed et al., 1996c). The epoxygenase pathway has been confirmed in cultured rat hippocampal astrocyte homogenate (Amruthesh et al., 1993; Stella et al., 1994b; Alkayed et al., 1996a). The generation of 20-hydroxyeicosatetraenoic acid (20-HETE) was increased after incubation with AA using rat cerebral vessel microsomes (Gebremedhin et al., 2000). The inhibition of 20-HETE synthesis ameliorated the reduction in cerebral blood flow followed by cortical spreading depression or subarachnoid hemorrhage in the rat (Kehl et al., 2002a). Furthermore, the inhibition of the epoxygenase pathway of AA reduced cerebral blood flow in vivo (Alkayed et al., 1996b). It was thus suggested that neuronal activation may lead to the release of astrocyte-derived AA metabolites to affect the functional neurovascular unit. David Attwell and Raymond C. Koehler et al. hypothesize that blood flow in the brain is regulated by neurotransmitter-mediated signaling via the AA pathways (Koehler et al., 2009; Attwell et al., 2010). Cytochrome P450 2C (CYP2C) and CYP4 A have been shown as epoxygenase and ω-hydroxylase involved in the production of EETs and HETEs from AA in heart, kidney, lung, and the liver (El-Sherbeni et al., 2013). However, CYP2C and CYP4 A were

Abbreviations: AA, arachidonic acid; EETs, epoxyeicosatrienoic acids; HETEs, hydroxyeicosatetraenoic acids; CYP, cytochrome P450; CREB, cAMP response element-binding protein; mGlu5 receptor, metabotropic glutamate receptor subtype 5; MAPK, mitogen-activated protein kinases; MPEP, 2-methyl-6-(phenylethynyl)-pyridine; DAPI, 4,6-diamidino-2-phenylindole; IOD, integrated option density; ChIP, chromatin immunoprecipitation; ACN, Analytical grade acetonitrile; EtOAc, ethyl acetate; BHT, 2,6-di-tert-butyl-4-methylphenol; L-AA, L(+)-ascorbicacid; FA, formic acid; CMPI, 2-chloro-1-methylpyridinium iodide; TEA, triethylamine; DMED, 2-dimethylaminoethylamine; CSD, cortical spreading depression; LSD, least significance difference

* Corresponding author at: No. 185 Donghu Road, Department of Pharmacology, Wuhan University School of Basic Medical Sciences, Wuhan, 430071, China.
E-mail address: yuejiang@whu.edu.cn (J. Yue).
[1] Equal contribution.

https://doi.org/10.1016/j.biocel.2019.03.001
Received 8 August 2018; Received in revised form 27 January 2019; Accepted 1 March 2019
Available online 08 March 2019
1357-2725/

present at lower levels or not observed in the human brain (Dutheil et al., 2009a). Do the neurotransmitters released from the neurons change AA epoxygenation and monooxygenation via astrocytic CYPs?

The previous study demonstrated that the main CYP isoforms present in the human brain included CYP46A1, 2J2, 2U1, 1B1, 2E1 and 2D6 (Dutheil et al., 2009b, 2010). CYP1B1 and CYP2U1 were found in the mitochondrial and microsomal fractions of astrocytes in the human frontal lobe, hippocampus, substantia nigra and cerebellum. In freshly isolated human brain microvessels, CYP1B1 and CYP2U1 were the only quantifiable CYP isoforms from the 21 CYPs investigated (Shawahna et al., 2011). The in vitro study reported that CYP1B1 preferentially produced midchain HETEs, almost 55% of its total metabolites (Choudhary et al., 2004). LC–MS analysis showed that CYP2U1 was able to metabolize long chain fatty acids including the metabolism of AA to 19- and 20-HETE (Chuang et al., 2004).

Glutamate is one of the most important neurotransmitters in the central nervous system. Previous study has shown the direct respond of the astrocytes to the glutamate released from synaptic terminals (Porter and McCarthy, 1996). Astrocytes have been recognized to sense glutamatergic synaptic activity over a large spatial domain. In the present study, we investigated the regulatory mechanism of brain CYP1B1 and CYP2U1 by glutamate and the changes in HETEs production in rat brain regions. This work adds to the current knowledge on the regulation of metabolic processes occurring in astrocytes by neurotransmitter-mediated signaling, and the pivotal role of astrocytes in the neurovascular unit.

2. Materials and methods

2.1. Animals and treatment

Adult Wistar rats (250–300 g) supplied by the Experimental Animal Center (Hubei, China) were kept in a room under a controlled temperature (22–25 °C), on a 12 h artificial light/dark cycle, with free access to food and water. All animal care and experimental procedures were approved by the Animal Care Committee of Wuhan University. The studies involving animals are reported in accordance with the ARRIVE guidelines for reporting experiments involving animals (McGrath et al., 2010; Kilkenny et al., 2010). After a 2-week accommodation period in our facilities, the animals were bred by randomly housing two females in a cage with one male rat. The litters were adjusted to 2 or 4 male pups per cage on the day of parturition. Age-matched pups were randomly divided into the monosodium L-glutamate group and the control group and subcutaneously injected with either monosodium L-glutamate (4 mg/g BW; Cat. 6106-04-3, Sigma-Aldrich, St. Louis, MO, USA) or an equivalent amount of saline at 1, 3, 5, and 7 days of age. Cortical spreading depression (CSD) has been thought as an excitability-related phenomenon, monosodium L-glutamate treatment (4 mg/g) in the developing rat brain has been used to establish the animal CSD model (Lima et al., 2013). Previous study has shown the activation of mitogen-activated protein kinases (MAPK) signaling pathway in rat hippocampus at 6~72 h after the last injection of monosodium L-glutamate (Ortuno-Sahagun et al., 2014). The rats were weaned at 25 days of age and sacrificed at 10 weeks after the injection. The brains were quickly removed, and the tissues for mRNA detection were stored in RNAlater according to the manufacturer's protocol (Ambion, Austin, TX). The samples for LC–MS/MS analysis were immediately frozen and stored at −80 °C.

2.2. Cell culture

Human glioma U251 cells (China Centre for Type Culture Collection, CCTCC, Wuhan, China) were incubated with glutamate (10–50 μM) for 24 h. The specific inhibitors of ERK (U0126, Cat. U120, Sigma-Aldrich, St Louis, MO, USA), p38 (SB202190, Cat. S8307, Sigma-Aldrich, St Louis, MO, USA), or JNK (SP600125, Cat. S5567, Sigma-Aldrich, St Louis, MO, USA) were pre-treated the cells for 30 min before the incubation with glutamate. The specific inhibitors of PKA (H 89 2HCl, Cat. S1582, Selleckchem, Houston, TX, USA) and PKC (Ro 31–8220, Cat. S7207, Selleckchem, Houston, TX, USA) were pre-treated the cells for 60 min before the incubation with glutamate. U251 cells were pre-treated with or without the selective mGluR5 antagonist, 2-methyl-6-(phenylethynyl)-pyridine (MPEP), for 30 min before the incubation with glutamate.

The brain microvascular endothelial cell line hCMEC/D3 (Shanghai Honsun Biological Technology Co., Ltd., China) has been wildly used as a useful model of the human blood-brain barrier, which was derived from human temporal lobe microvessels isolated from tissue excised during surgery for control of epilepsy (Weksler et al., 2013). The hCMEC/D3 cells were incubated with glutamate (10–50 μM) for 24 h.

The brains of neonatal (0–3 days) Wistar rats were isolated for the primary astrocyte culture as previously described (Fenghong et al., 2012). Briefly, the tissues were washed with ice-cold PBS for three times and then digested with 0.25% (w/v) trypsin solution (pH 7.4). The cells were transferred into DMEM with 10% (v/v) FBS containing penicillin and streptomycin. The samples were filtered using mesh screens and diluted to a final density of 1×10^6/ml. After seeding in the culture dishes pre-coated with poly-D-lysine, the astrocytes were isolated by differential adhesion method. The media was replaced every 3 days, and the oligodendrocytes were removed by shaking the dishes for 15 h on the day 12. The obtained primary astrocytes were grown for 5 days, and then re-plated in a culture dish for the identification.

2.3. Real-time RT-PCR

Total RNA was isolated using TRIzol reagent (Cat. 108952, Invitrogen, Carlsbad, CA, USA) according to the manufacturer's protocol. cDNA was synthesized using a cDNA synthesis kit (TOYOBO, Osaka, Japan) and the real-time PCR reactions with SYBR Green (Cat. K1621, TOYOBO, Osaka, Japan) were performed on a CFX connect real-time PCR detection system (Bio-Rad, Hercules, CA, USA). GAPDH was used for the normalization of relative expression levels. Gene expression levels were calculated using the $2-\Delta\Delta CT$ method relative to the internal control. Primers are listed in Supplementary Table S1.

2.4. Immunoblotting

The total proteins (20 μg) from U251 cells were separated by SDS-polyacrylamide gel electrophoresis (4% stacking and 10% separating gels). The samples were transferred onto PVDF membranes and incubated for 2 h with a polyclonal rabbit anti-human CYP1B1 (ab33586 1:1500, Abcam, Cambridge, MA, USA) or a polyclonal rabbit anti-human CYP2U1 antibody (ab65128 1:1000, Abcam, Cambridge, MA, USA). For normalization of protein levels, β-actin (sc-47778 1:1000, Santa Cruz Biotechnology, Santa Cruz, CA, USA) was used as a loading control. The blots were then incubated with the peroxidase-conjugated goat anti-rabbit antibody (Cat.12–348, 1:3000, Millipore, Billerica, MA, USA) for 1 h. The blots were visualized using chemiluminescence followed by exposure to autoradiography film (Kodak X-OMAT, Kodak, Rochester, NY, USA) and digitalized using a CCD camera (Beijing Liuyi Instruments, Beijing, China). The blots were analyzed using the MCID Elite software (InterFocus Imaging Ltd., Linton, UK), and the baseline density of each band was subtracted from the density peak.

2.5. Fluorescent immunocytochemistry

U251 cells were fixed with 4% paraformaldehyde for 20 min, and then permeabilized with 0.5% Triton X-100 for 10 min. Fixed cells were blocked with 3% fetal calf serum for 30 min. The cells were incubated with a monoclonal rabbit anti-human phospho-CREB (S133) antibody (Cat. ab32096, 1:100, Abcam, Cambridge, UK) and a goat anti-mouse alpha tubulin antibody (Cat. 66031-1-lg, 1:100, Proteintech Group,

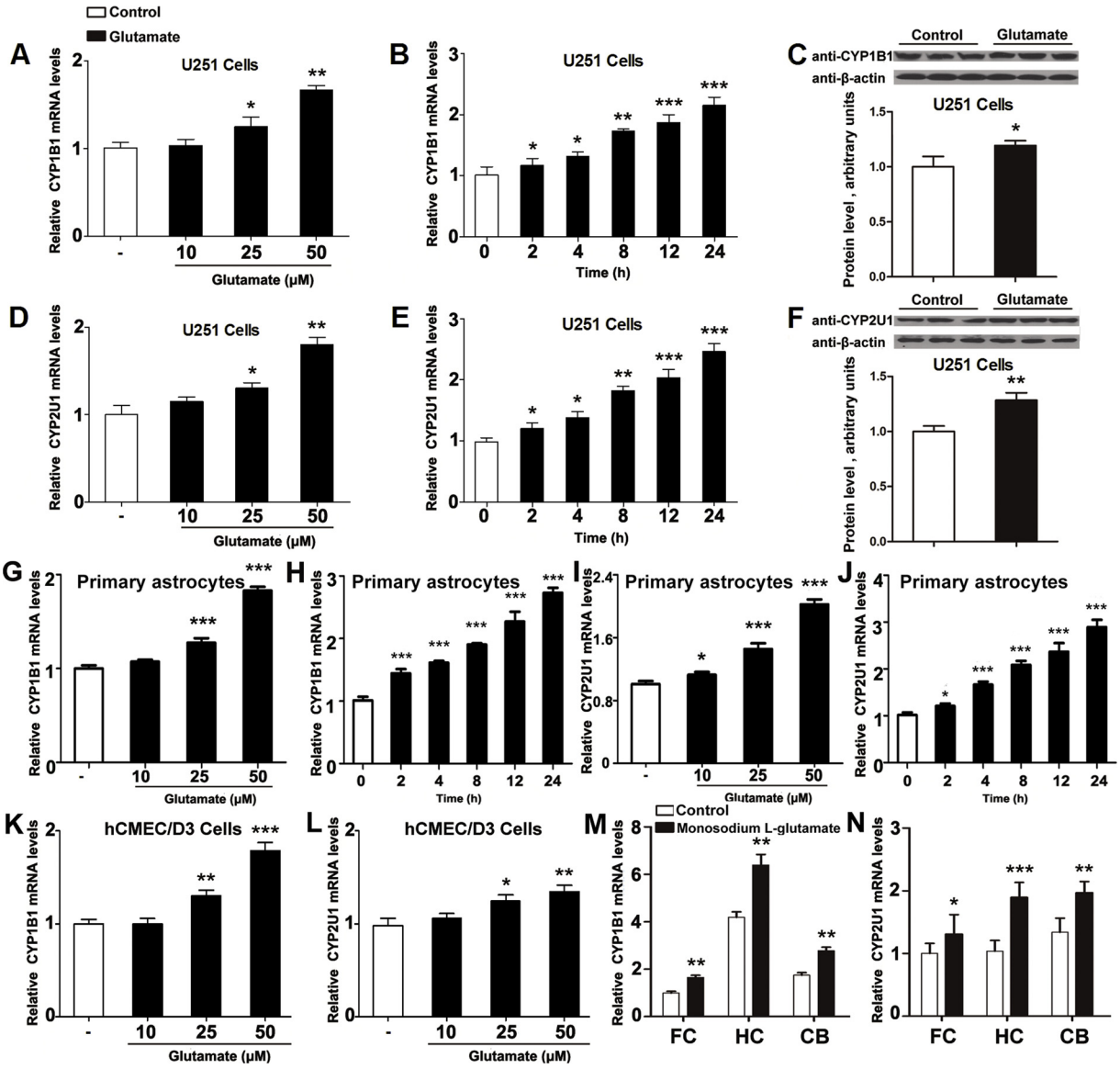

Fig. 1. Glutamate induced CYP1B1 and CYP2U1 expression levels in vitro and in vivo. Glutamate increased CYP1B1 (A) and CYP2U1 (D) mRNA levels in a dose-dependent manner after the treatment for 8 h in U251 cells. The initial increases in CYP1B1 (B) and CYP2U1 (E) mRNA levels were observed at 2 h after the glutamate treatment (50 μM) in U251 cells. Compared with the control, the protein levels of CYP1B1 (C) and CYP2U1 (F) were increased in U251 cells treated with 50 μM of glutamate for 24 h. The mRNA levels of CYP1B1 (G) and CYP2U1 (I) in primary astrocytes were dose-dependently up-regulated following glutamate exposure. The maximal induction in CYP1B1 (H) and CYP2U1 (*J*) levels by glutamate (50 μM) were observed at 24 h in the astrocytes.The mRNA levels of CYP1B1 (K) and CYP2U1 (L) were dose-dependently increased after the glutamate treatment for 8 h in hCMEC/D3 cells. The mRNA levels of CYP1B1 (M) and CYP2U1 (N) were higher in the frontal cortex (FC), hippocampus (HC), and cerebellum (CB) in rats treated with monosodium L-glutamate at 1, 3, 5, and 7 days of age. The data are mean ± S.D.; $n = 3$ per group; * $p < 0.05$, ** $p < 0.01$ and *** $p < 0.001$ versus the respective control.

Chicago, IL, USA) overnight at 4 °C. The samples were then incubated with a goat anti-rabbit fluorescein isothiocyanate for phospho-CREB (Cat. AS1110, 1:100, Aspen Biotechnology, Wuhan, China) and a Cy3-labeled goat anti-rat secondary antibody for alpha tubulin (Cat. AS1111, 1:100, Aspen Biotechnology, Wuhan, China) in PBS for 1 h at 37 °C. Then the cells were washed twice in PBS and incubated with 4,6-diamidino-2-phenylindole (DAPI) for 5 min. The images were analyzed under fluorescence microscopy (Olympus Corporation, Tokyo, Japan). Identical illumination and camera settings were used within each data set.

2.6. Chromatin immunoprecipitation (ChIP) assays

ChIP assays were performed using a kit (Epigentek Group Inc., Brooklyn, NY, USA) according to the manufacturer's protocol. Briefly, the cross-linked chromatin of the nuclear fractions was sheared by sonication to within a specific range of fragment lengths. Approximately 10% of the chromatin was retained as the input material. The chromatin solution was immunoprecipitated with an anti-CREB antibody or a non-immune rabbit IgG as a negative control. The Transcription Element Search Software (MatInspector; Genomatix) was employed to identify putative transcription factor binding sites in the *CYP1B1* and *CYP2U1* promoters. The immunoprecipitated DNA was retrieved and then purified using a PCR cleanup kit (Axygen, USA). PCR was performed with DNA isolated from both an aliquot of the total nuclear extraction (input) and the immunoprecipitated complex. The number of cycles used to amplify the PCR products (primers are listed in Table S1) was within the linear range. Products were resolved on 2% agarose gel. The band intensities were quantitated by the AutoChemi Imaging System (UVP LLC, Upland, CA, USA).

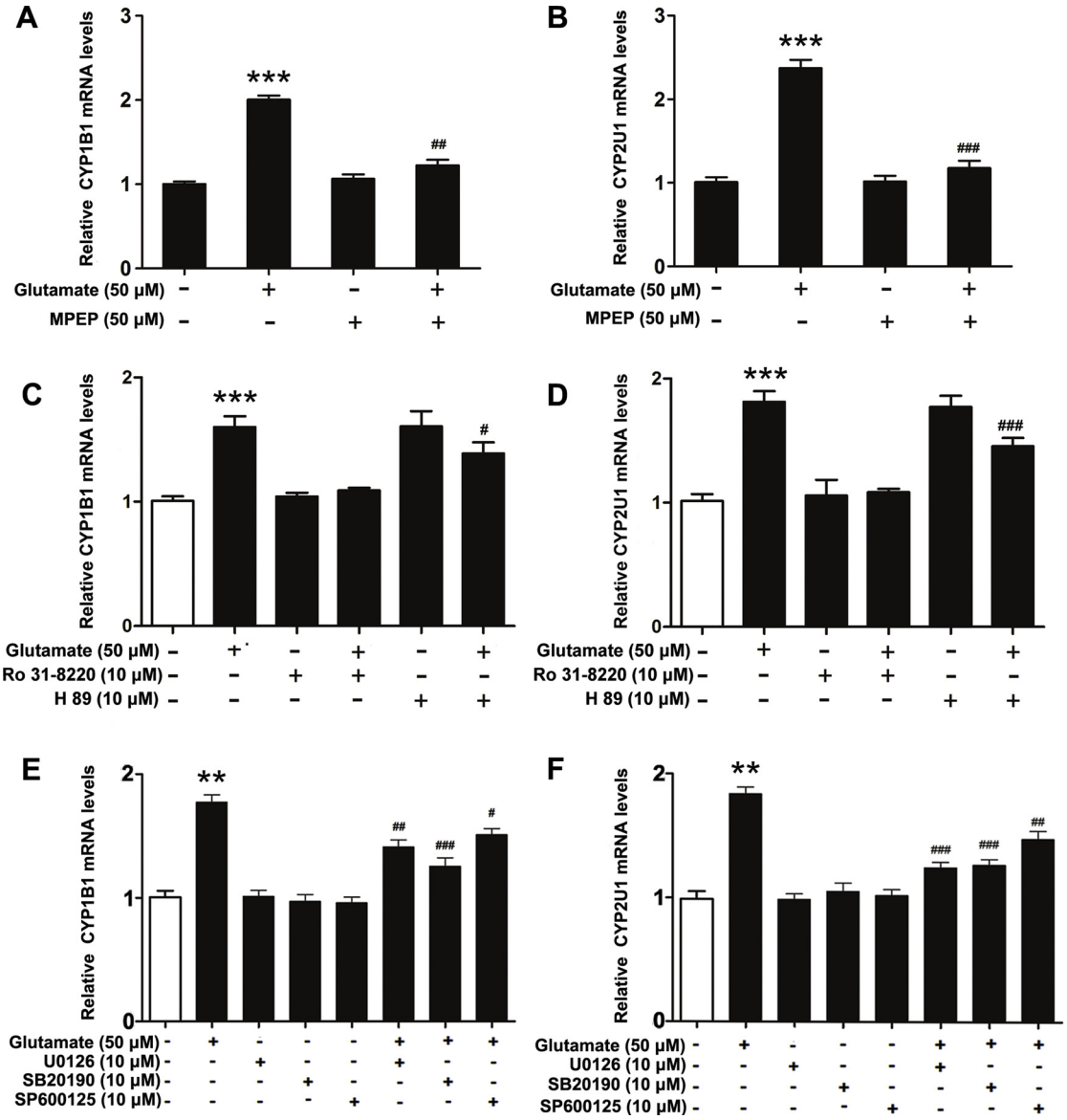

Fig. 2. mGlu5 receptor mediated the up-regulation of CYP1B1 and CYP2U1 levels by glutamate in U251 cells. The selective mGluR5 antagonist, 2-methyl-6-(phenylethynyl)-pyridine (MPEP), abolished the glutamate-induced up-regulation of CYP1B1 (A) and CYP2U1 (B) mRNA levels. The inhibition of PKA by H 89 attenuated the glutamate-induced increases in the mRNA levels of CYP1B1 (C) and CYP2U1 (D), but there was no change in the levels of CYP1B1 and CYP2U1 in the cells pre-treated with the inhibitor of PKC (Ro 31–8220) before the incubation with glutamate. The inhibitors of ERK1/2 (U0126), p38 (SB202190), and JNK (SP600125) attenuated the induction of CYP1B1 (E) and CYP2U1 (F) mRNA levels after glutamate treatment. The data are mean ± S.D.; $n = 3$ per group; ** $p <$ 0.01 and *** $p < 0.001$ versus the respective vehicle-treated controls; $^{\#}p <$ 0.05, $^{\#\#}p < 0.01$ and $^{\#\#\#}p < 0.001$ versus the glutamate group.

2.7. Plasmid construction

The XhoI (Cat. ER0692, Thermo Scientific, Waltham, MA, USA)/HindIII (Cat. ER0505, Thermo Scientific, Waltham, MA, USA) fragments of the human *CYP1B1* (corresponding to -1463 bp to -1927 bp) and *CYP2U1* (corresponding to -1690 bp to -1960 bp) promoter regions were subcloned into the XhoI/HindIII-digested pGL4.11 vector (Invitrogen, Carlsbad, CA, USA). The fragments encoding the CREB were cloned into the pFLAG-CMV (-) vector (Invitrogen, Carlsbad, CA, USA) following digestion with EcoRI (Cat. ER1921, Thermo Scientific, Waltham, MA, USA)/BamHI (Cat. ER0505, Thermo Scientific, Waltham, MA, USA). The forward primers for the deletion constructs of the *CYP1B1* and *CYP2U1* promoters and the amplification of CREB are listed in Supplementary Table S2. All final constructs were verified by DNA sequence analysis.

2.8. Luciferase assays

U251 cells were transiently co-transfected with luciferase reporter plasmids of *CYP1B1* and *CYP2U1* promoter regions, CREB expression vector (pFLAG-CMV) or with an empty vector. A dual-luciferase reporter assay was performed according to the manufacturer's instructions (Promega, Madison, WI, USA). Luciferase activity was quantified 48 h after transfection using a luminometer and the Stop & GloH Dual Luciferase Kit (Promega, Madison, WI, USA). Firefly luciferase activity was corrected according to Renilla luciferase activity to control for transfection efficiency.

2.9. Fluorescent immunohistochemistry

To investigate the effects of glutmate on CYP1B1 and CYP2U1 protein levels across the brain regions, the tissues were fixed with 4% paraformaldehyde and embedded in paraffin. The antigen retrieval was

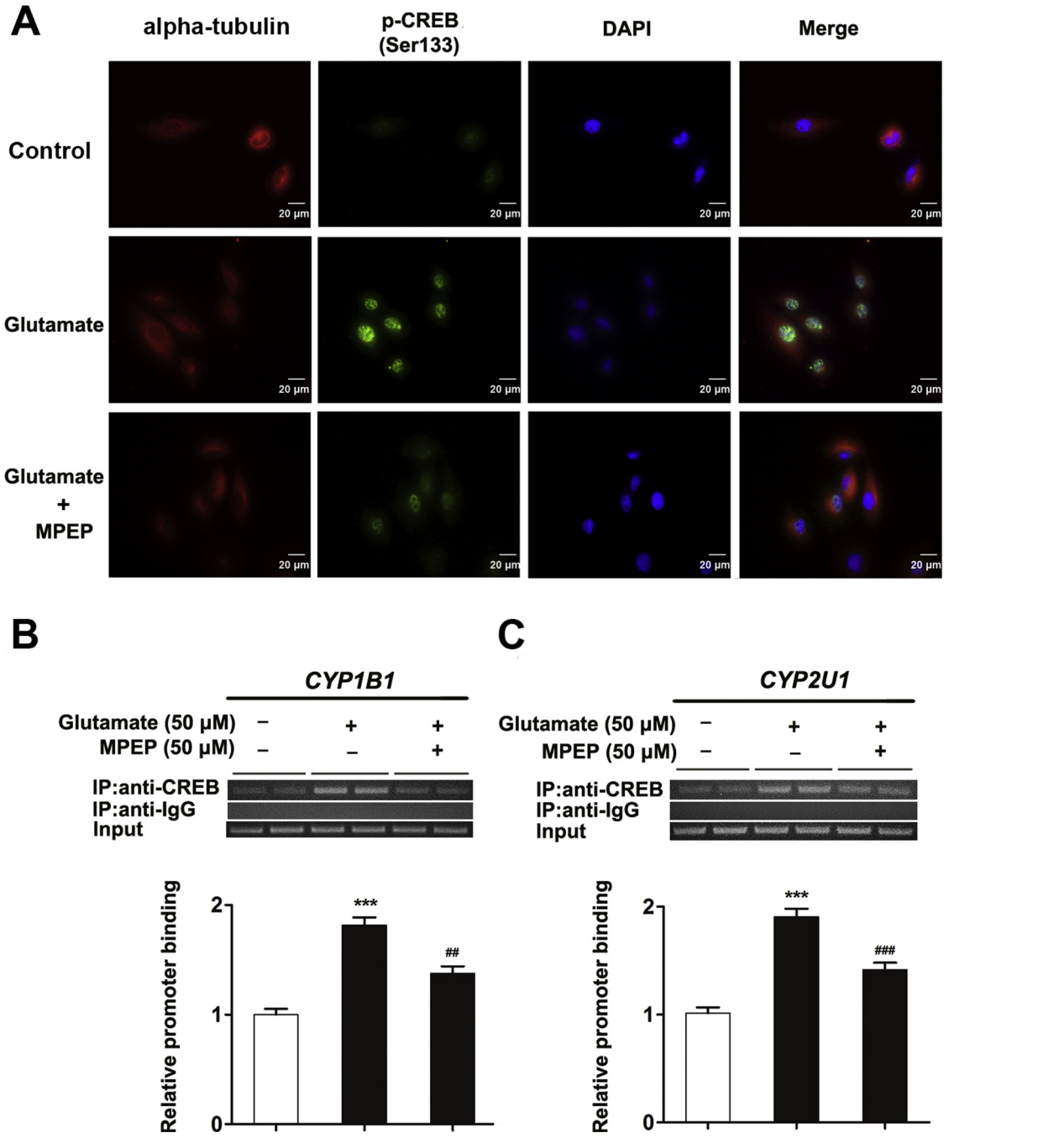

Fig. 3. mGlu5 receptor blockade decreased the glutamate-induced phosphorylation of CREB protein binding to *CYP1B1* and *CYP2U1* promoters in U251 cells. Fixed cells were labeled with the antibody against alpha-tubulin (red), and nuclei were counterstained with DAPI (blue). Glutamate treatment increased the levels of phosphorylated CREB at Ser133 (green) in the nuclear (A). The selective mGluR5 antagonist, 2-methyl-6-(phenylethynyl)-pyridine (MPEP), inhibited the activation of p-CREB induced by glutamate in the nuclear. The increases in the binding of CREB with the *CYP1B1* (B) and *CYP2U1* (C) promoters determined by ChIP assay following glutamate treatment was attenuated by MPEP. The data are mean ± S.D.; $n = 3$ per group; $^{***}p < 0.001$ versus the respective vehicle-treated controls; $^{\#\#}p < 0.01$ and $^{\#\#\#}p < 0.001$ versus the glutamate group (For interpretation of the references to colour in this figure legend, the reader is referred to the web version of this article).

performed with citrate buffer (0.1 M, pH 6.0) after deparaffinization and rehydration. The samples were incubated with a polyclonal rabbit anti-rat CYP1B1 antibody (1:300), a polyclonal rabbit anti-rat CYP2U1 antibody (1:300), or a monoclonal mouse anti-rat GFAP antibody (Cat. 60190-1-Ig, 1:500, Proteintech, Wuhan, China) following the incubation with 3% BSA for 1 h. The secondary antibodies were a goat anti-rabbit CY3 (Cat. AS1109, 1:100, Aspen Biotechnology, Wuhan, China) for CYP1B1 and CYP2U1, or a Goat anti-mouse fluorescein isothiocyanate for phospho-CREB (Cat. AS1112, 1:100, Aspen Biotechnology, Wuhan, China). Images were observed using an Olympus BX51 fluorescent microscope (Olympus Corporation, Tokyo, Japan) equipped with a digital camera (DP 72 Olympus). Identical illumination and camera settings were used within each data set. The integrated option density (IOD) was calculated automatically with Image J (National Institutes of Health, Bethesda, MD, USA). The area of the positive labeling by both anti-GFAP antibody and anti-CYP1B1 or anti-CYP2U1 antibody was automatically calculated to indicate the levels of CYP1B1 or CYP2U1 protein in the astrocytes.

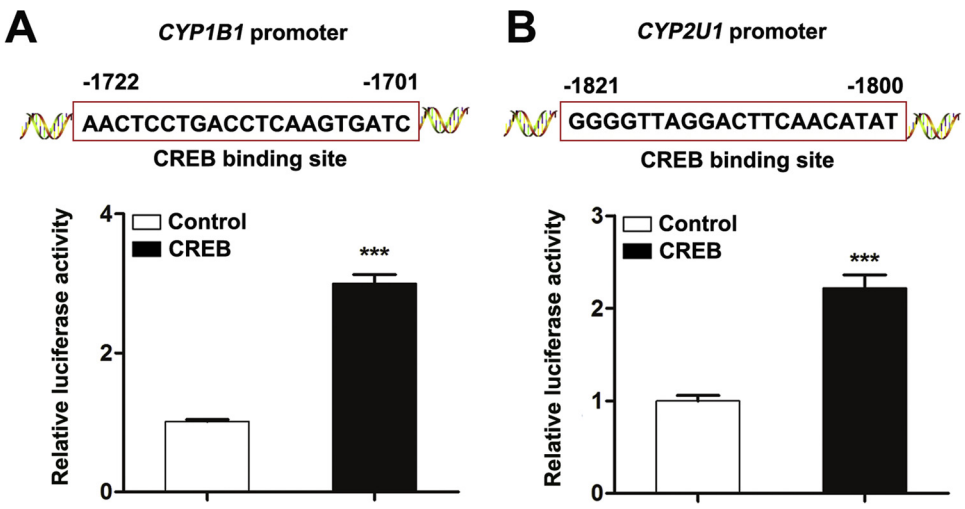

Fig. 4. The activation of the *CYP1B1* and *CYP2U1* promoters by CREB proteins was detected by luciferase assays. The predicted binding sites of *CYP1B1* (A) and *CYP2U1* (B) promoters were shown. Basal activity levels measured in cells transfected with the pFLAG-CMV empty vector were set to 1. The data are mean ± S.D.; $n = 3$ per group; $^{***}p < 0.001$ versus the respective control.

Table 1
Fluorescent Immunohistochemical analysis of the induction of brain CYP1B1 proteins by monosodium L-glutamate.

	Control	Glutamate
Cortex		
Layer I	±	+
Layer II-V	+ + +	+ + + +
Layer VI	±	±
Hippocampus		
Dentate gyrus	+	+
CA1,CA2,CA3	+ +	+ + +
Cerebellum		
Molecular layer	±	+
Granular layer	+ + +	+ + + +
White matter	+ +	+ + +
Brainstem	±	±
Substantia nigra	+	+

The integrated option density (IOD) analyzed by Image *J*. ±, 0 < IOD ≤ 100; +, 100 < IOD ≤ 1000; + +, 1000 < IOD ≤ 3000; + + +, 3000 < IOD ≤ 5000; + + + +, IOD > 5000.

2.10. UPLC-ESI-MS/MS analysis

All the epoxyeicosanoids, including 5-HETE, 8-HETE, 11-HETE, 12-HETE, 15-HETE, 16-HETE, 18-HETE, 19-HETE, and 20-HETE, were purchased from Cayman Chemical (Arbor, MI, USA). Analytical grade acetonitrile (ACN), ethyl acetate (EtOAc), 2,6-di-tert-butyl-4-methylphenol (BHT), L(+)-ascorbicacid (L-AA), formic acid (FA), 2-chloro-1-methylpyridinium iodide (CMPI), triethylamine (TEA), and 2-dimethylaminoethylamine (DMED) were supplied by Sinopharm Chemical Reagent Co., Ltd. (Shanghai, China). The generation of HETEs in rat brain regions was determined as previously described (Zhu et al., 2015). Briefly, the homogenized brain tissue was extracted using extraction solvent (EtOAc) containing BHT and FA. The extracted sample was redissolved and added with CMPI and TEA. DMED or d_4-DMED was added to label HETEs after vortexing for 5 min. UPLC analysis was performed on a Shimadzu LC-30AD UPLC (Tokyo, Japan) with an Acquity UPLC BEH phenyl column (2.1 mm × 50 mm, 1.7 m, Waters). The mobile phase consisted of FA in water (0.1%, v/v) and ACN/MeOH (7/3, v/v). The flow rate of the mobile phase was 0.4 mL/min with a gradient elution. Mass spectrometry analysis was performed on an ABI/SCIEX 4500 Triple Quad™with a Turbo V ion source, and the samples were detected in positive ion mode. Curtain gas (CUR), nebulizer gas (GS1), and turbo-gas (GS2) were set at 8, 35, and 30 psi, respectively. Nebulizer gas and heater gas were set at 50 and 60 psi, respectively. The electrospray voltage was 5000 V, and the turbo ion spray source temperature was 500 °C. The analysis was performed in multiple reaction monitoring (MRM) mode, and data acquisitions were performed using Analyst 1.6.1 software (Applied Biosystems).

2.11. Statistical analyses

The mRNA and protein levels were expressed as arbitrary units (mean ± S.D.). The cell data were collected from at least 3 independent cell preparations. The quantity of HETEs was calculated using the peak area ratios (the metabolite/its own internal standard). The differences in mRNA, protein, and HETEs between the treatment groups were assessed by one-way ANOVA or one-way ANOVA followed by least significant difference (LSD) post hoc tests. Differences with $p < 0.05$ were considered significant.

3. Results

3.1. Glutamate induces CYP1B1 and CYP2U1 expression levels in cells and rats

Previous report showed the extrasynaptic glutamate concentration can reach 190 μM in Bergmann glia in the cerebellum (Lewerenz and Maher, 2015). Approximately 80% of all glutamate released from neurons is taken up by astrocytes, and astrocytes have also been found to release glutamate by several different mechanisms (e.g. plasma membrane glutamate transporters, volume-regulated anion channels) (Rose et al., 2013). CYP1B1 and CYP2U1 mRNA levels were dose-dependently induced by glutamate treated for 8 h in U251 cells. Compared with the control, 50 μM of glutamate respectively increased CYP1B1 and CYP2U1 mRNA levels by 1.68-fold ($p < 0.01$) and 1.80-fold ($p < 0.01$) in U251 cells (Fig. 1A, D). The initial increases in CYP1B1 and CYP2U1 mRNA levels were observed at 2 h after the glutamate treatment (50 μM) in U251 cells (Fig. 1B, E). The protein levels of CYP1B1 and CYP2U1 were increased by 1.20-fold ($p < 0.05$) and 1.28-fold ($p < 0.01$) after glutamate incubation for 24 h (Fig. 1C, F). The induction of CYP1B1 and CYP2U1 mRNA levels by glutamate in primary astrocytes was in a dose- and time-dependent manner. Compared with the control, 50 μM of glutamate respectively increased CYP1B1 and CYP2U1 mRNA levels by 1.83-fold ($p < 0.001$) and 2.02-fold ($p < 0.001$) in the astrocytes (Fig. 1G, I). The maximal induction of CYP1B1 and CYP2U1 levels was observed at 24 h after the glutamate treatment (50 μM) in the cells (Fig. 1H, J). In addition, CYP1B1 and CYP2U1 mRNA levels were increased by 1.79-fold ($p < 0.001$) and 1.34-fold ($p < 0.01$) in hCMEC/D3 cells (Fig. 1K,L).

The blood-brain-barrier is not fully developed before the weaning stage in the rats, and subneurotoxic doses of monosodium L-glutamate

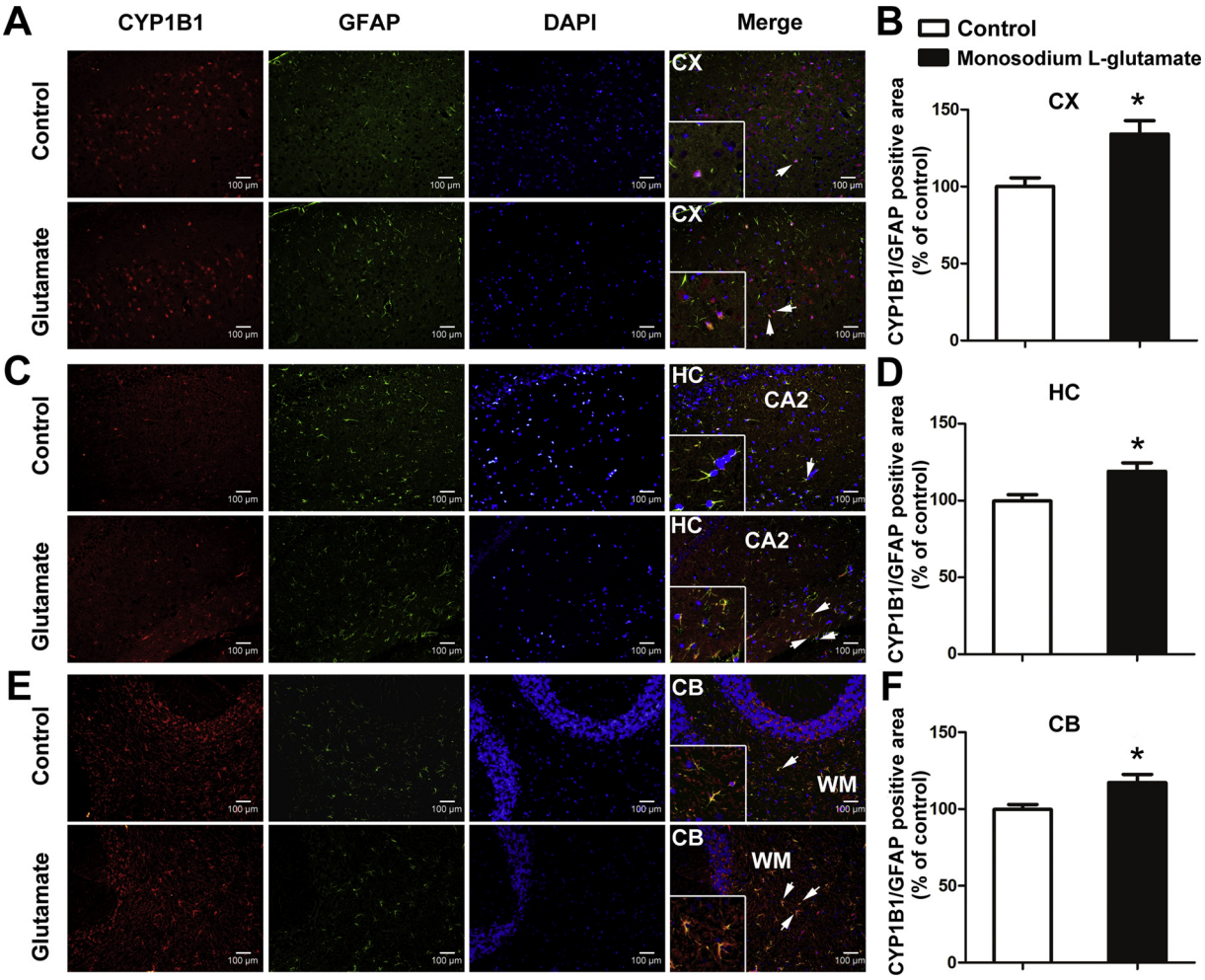

Fig. 5. Changes in the CYP1B1 proteins in the brain regions from rats treated with monosodium L-glutamate at 1, 3, 5, and 7 days of age. The tissues were labeled with the antibodies against CYP1B1 (red) and GFAP (green), and nuclei were counterstained with DAPI (blue). The fluorescent intensity of CYP1B1 was stronger in the cortex (CX) in monosodium L-glutamate group, compared with the controls (A); the staining was stronger in the cells of CA2 in the hippocampus (HC) in monosodium L-glutamate group (C); in the cerebellum (CB), staining was stronger in glial cells in the white matter (WM) following monosodium L-glutamate treatment (E). The co-localization area labeled by both anti-CYP1B1 antibody and anti-GFAP antibody was increased in the cortex (B), hippocampus (D), and the cerebellum (F) after the treatment of monosodium L-glutamate, compared with the controls. The data are mean ± S.D.; $n = 3$ per group; *$p < 0.05$ versus the respective control (For interpretation of the references to colour in this figure legend, the reader is referred to the web version of this article).

Table 2
Fluorescent Immunohistochemical analysis of the induction of brain CYP2U1 proteins by monosodium L-glutamate.

Brain region	Control	Glutamate
Cortex		
Layer I	±	±
Layer II-V	+ +	+ + +
Layer VI	±	+
Hippocampus		
Dentate gyrus	±	+
CA1,CA2,CA3	+	+ +
Cerebellum		
Molecular layer	±	±
Granular layer	+ +	+ + + +
White matter	+	+ +
Brainstem	±	±
Substantia nigra	+	+ +

The integrated option density (IOD) analyzed by Image *J*. ± , 0 < IOD ≤ 100; +, 100 < IOD ≤ 1000; + +, 1000 < IOD ≤ 3000; + + +, 3000 < IOD ≤ 5000; + + + +, IOD > 5000.

could result in subtle, prolonged alterations in the basal levels of the glutamate system (Lima et al., 2013). Compared with the control group, the CYP1B1 mRNA levels were significantly increased in the frontal cortex (1.65-fold), hippocampus (1.53-fold), and cerebellum (1.58-fold) from adult rats that received a subcutaneous injection of monosodium L-glutamate at 1, 3, 5, and 7 days of age (Fig. 1M). The increases in CYP2U1 mRNA levels were also observed in the frontal cortex (1.31-fold), hippocampus (1.82-fold), and cerebellum (1.47-fold) from glutamate-treated rats (Fig. 1N).

3.2. mGlu5 receptor blockade attenuates the up-regulation of CYP1B1 and CYP2U1 levels by glutamate in U251 cells

Compared with the control, the mRNA levels of CYP1B1 and CYP2U1 were increased after glutamate treatment for 24 h; however, the MPEP pretreatment abolished the induction of CYP1B1 and CYP2U1 by glutamate (Fig. 2A, B). Compared with the glutamate group, the PKA inhibitor (H 89) reduced the glutamate-induced CYP1B1 and CYP2U1 mRNA levels by 13.8% ($p < 0.05$) and 20% ($p < 0.001$); however, there was no significant change in CYP1B1 and CYP2U1 mRNA levels in cells exposed to glutamate following the pretreatment of the PKC inhibitor (Ro 31–8220) (Fig. 2C, D). Compared with the glutamate group,

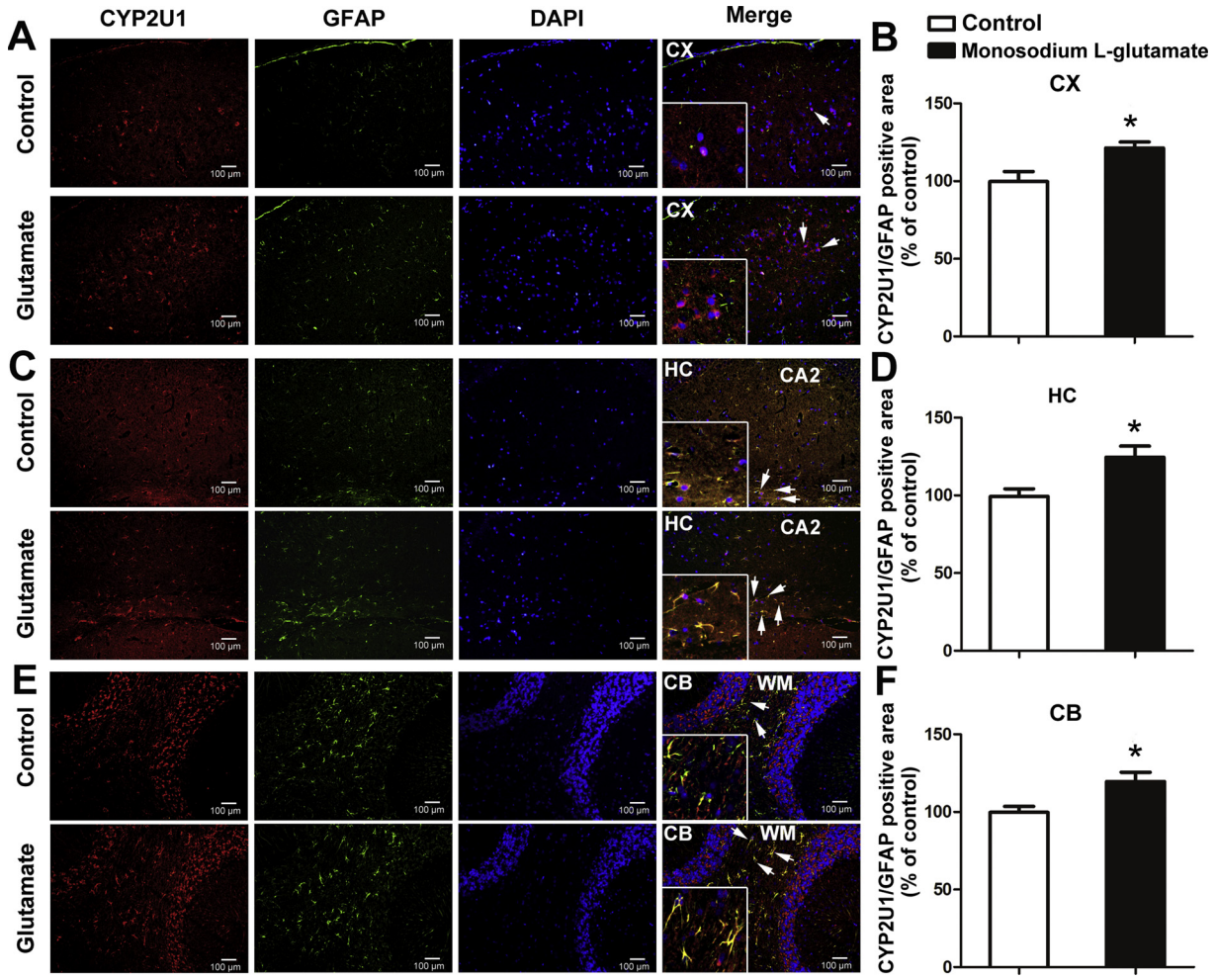

Fig. 6. Changes in the CYP2U1 proteins across the brain regions from rats treated with monosodium L-glutamate at 1, 3, 5, and 7 days of age. The tissues were labeled with the antibodies against CYP1B1 (red) and GFAP (green), and nuclei were counterstained with DAPI (blue). The fluorescent intensity of CYP2U1 was stronger in the cortex (CX) in monosodium L-glutamate group, compared with the controls (A); the staining was stronger in the cells of CA2 in the hippocampus (HC) in monosodium L-glutamate group (C); in the cerebellum (CB), the staining was stronger in glial cells in the white matter (WM) after monosodium L-glutamate treatment(E). The co-localization area labeled by both anti-CYP2U1 antibody and anti-GFAP antibody was increased in the cortex (B), hippocampus (D), and the cerebellum (F) after the treatment of monosodium L-glutamate, compared with the controls. The data are mean ± S.D.; $n = 3$ per group; $^{*}p < 0.05$ versus the respective control (For interpretation of the references to colour in this figure legend, the reader is referred to the web version of this article).

the specific inhibitors of ERK (U0126), p38 (SB202190), and JNK (SP600125) respectively decreased glutamate-induced CYP1B1 mRNA levels by 20% ($p < 0.01$), 29% ($p < 0.001$) and 15% ($p < 0.05$) (Fig. 2E). Meanwhile, the glutamate-induced CYP2U1 mRNA levels were inhibited by the specific inhibitors of ERK, p38, and JNK by 32% ($p < 0.001$), 36% ($p < 0.001$), 20% ($p < 0.01$), compared with the glutamate group (Fig. 2F). The data suggest the involvement of PKA and MAPK signaling pathways in the induction of astrocytic CYP1B1 and CYP2U1 by glutamate via mGlu5 receptor.

3.3. mGlu5 receptor blockade decreases the glutamate-induced phosphorylation of CREB protein in the nuclear and the CREB-mediated activation of CYP1B1 and CYP2U1 promoters in U251 cells

Compared with the control, the increases in the phosphorylated CREB protein (green) in the nuclear (blue) was seen at 30 min in cells (red) after glutamate treatment; however, the MPEP pretreatment significantly inhibited the induction of the phosphorylated CREB protein by glutamate (Fig. 3A). The ChIP assay showed that the binding of CREB protein with the *CYP1B1* and *CYP2U1* promoters were increased by 1.80-fold ($p < 0.001$) and 1.94-fold ($p < 0.001$) by glutamate treatment for 24 h compared with the control (Fig. 3B, C). The MPEP pretreatment attenuated the induction of the binding of CREB protein with the *CYP1B1* and *CYP2U1* promoters by glutamate. The data from the luciferase assay indicated that CREB activated the *CYP1B1* promoter located at -1722 bp to -1701 bp, and *CYP2U1* promoter located at -1821 bp to -1800 bp (Fig. 4A, B).

3.4. Changes in the protein levels of CYP1B1 and CYP2U1 by glutamate in rats

The fluorescent immunohistochemistry data confirmed the up-regulation of brain CYP1B1 and CYP2U1 by glutamate. Compared with control animals, CYP1B1 immunostaining was more intense in the layer II - V of the cortex, the CA1 - CA3 of the hippocampus, and the granular layer and white matter of the cerebellum following monosodium L-glutamate treatment (Table 1, Fig. 5); meanwhile, CYP2U1 protein levels were also higher in the layer II - V of the cortex, the CA1 - CA3 of the hippocampus, the granular layer and white matter of the cerebellum, and the substantia nigra after monosodium L-glutamate treatment (Table 2, Fig. 6). The co-localization assay indicated that both CYP1B1 and CYP2U1 proteins were present not only in the astrocytes, but also in the neurons. The positive area labeled by both anti-CYPs antibody and anti-GFAP antibody calculated by Image J showed that

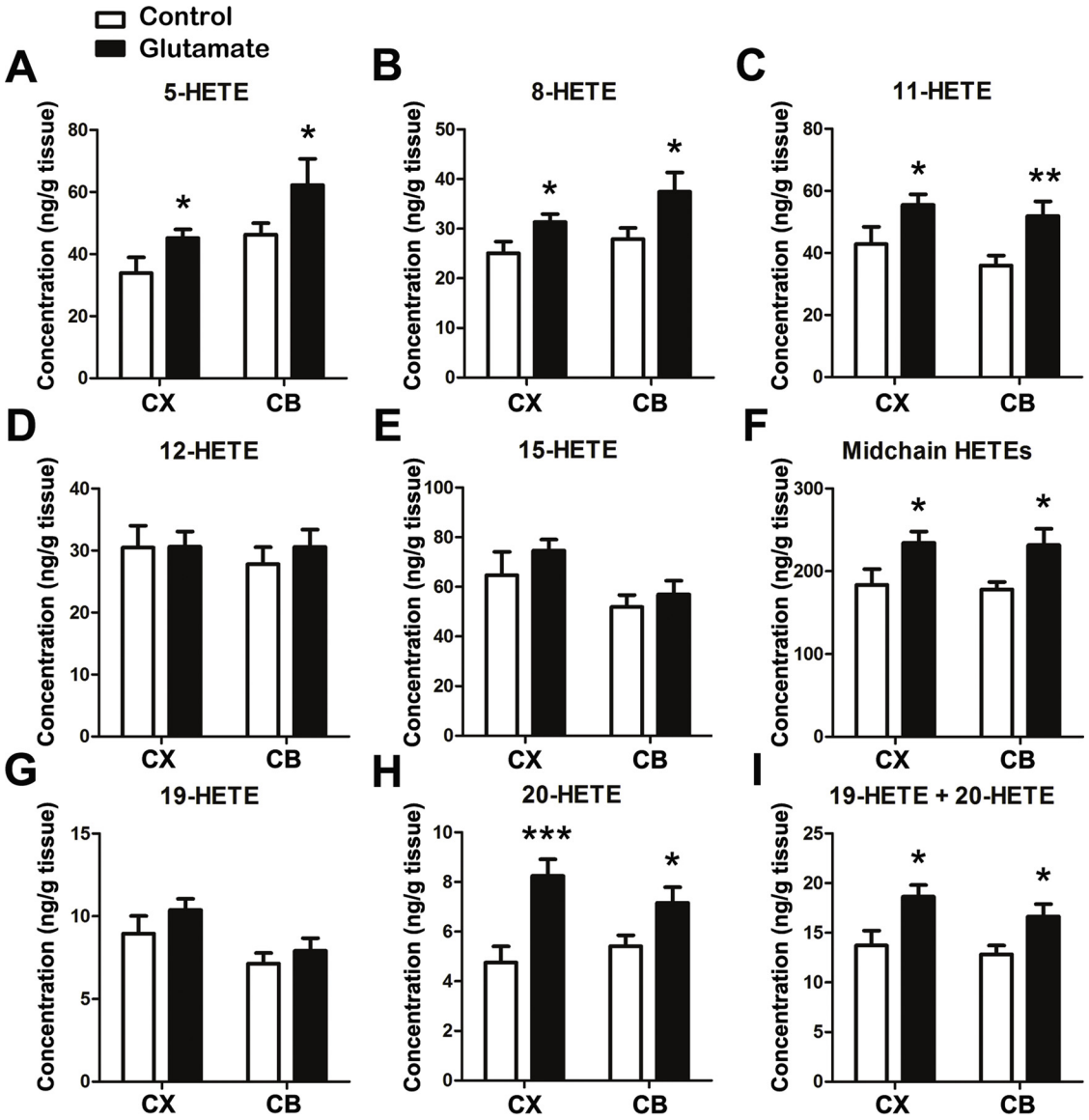

Fig. 7. Changes in the production of hydroxyicosatetraenoic acids (HETEs) in the brain regions from rats treated with monosodium L-glutamate at 1, 3, 5, and 7 days of age. Compared with the control, the generation of 5-HETE (A), 8-HETE (B), and 11-HETE (C) was increased in the cortex (CX) and the cerebellum (CB) by monosodium L-glutamate. The total production of the mid-chain HETEs in the cortex and the cerebellum was increased by the treatment of monosodium L-glutamate compared with the controls (F), although there was no change of the production 12-HETE (D), and 15-HETE (E). Compared with the control, the production of 20-HETE was increased in the cortex and the cerebellum from glutamate-treated rats (H). Glutamate increased the total production of the terminal HETEs in the cortex and the cerebellum compared with the controls (I), although there was no change of the generation of 19-HETE after the treatment of monosodium L-glutamate (G). n = 8 per group; *p < 0.05, **p < 0.01 and ***p < 0.001 versus the respective control.

astrocytic CYP1B1 (Fig. 5B, D, F) and CYP2U1 (Fig. 6B, D, F) proteins were increased by monosodium L-glutamate treatment.

3.5. Changes in the production of HETEs by glutamate in rats

Glutamate increased the total production of the mid-chain HETEs, generated by CYP1B1 from AA, in the cortex and the cerebellum after the treatment of monosodium L-glutamate (Fig. 7F). Compared with the control, 5-HETE, 8-HETE, and 11-HETE were respectively increased by 1.33-fold ($p < 0.05$), 1.25-fold ($p < 0.05$), and 1.29-fold ($p < 0.05$) in the cortex from rats treated with monosodium L-glutamate; additionally, 5-HETE, 8-HETE, and 11-HETE were respectively increased by 1.34-fold ($p < 0.05$), 1.34-fold ($p < 0.05$), and 1.46-fold ($p < 0.01$) in the cerebellum (Fig. 7A - C). The treatment of monosodium L-glutamate induced the total production of 19- and 20-HETE, produced by CYP2U1 from AA, in the cortex and the cerebellum (Fig. 7I). The previous study has shown that microsomal preparations from Sf9 cells transfected with pVL-CYP2U1 vector preferentially metabolize AA to 20-HETE (Chuang et al., 2004). Compared with the control, 20-HETE was respectively increased by 1.73-fold ($p < 0.001$) in the cortex and 1.32-fold ($p < 0.05$) in the cerebellum from glutamate-treated rats (Fig. 7H). The changes in the production profile of HETEs in the cortex and cerebellum can be due to the regulation of CYP1B1 and CYP2U1 in both neurons and astrocytes in the microenvironment respond to the neurotransmitter.

4. Discussion

This study demonstrated that mGlu5 receptor mediated the regulation of brain CYP1B1 and CYP2U1 by glutamate, and that glutamate changed the HETEs production within the brain. We showed that glutamate up-regulated brain CYP1B1 and CYP2U1 via CREB. Our

previous work showed that glutamate affects the production of epoxyeicosanoids via brain CYP2J (Liu et al., 2017). The alteration of the CYP-mediated AA metabolism in the brain by the neurotransmitter-mediated signaling support the hypothesis that neurons and/or astrocytes may play an important role in the autoregulation of cerebral blood flow. The previous studies demonstrated that the alteration of both HETEs and EETs synthesis affected cerebral blood flow in the rat (Kehl et al., 2002b; Alkayed et al., 1996a). Brain CYPs may be the important mediators in the autoregulation of the cerebral blood flow by neurotransmitters.

A sustained induction of brain CYP1B1 and CYP2U1 were observed in the cortex, hippocampus, and cerebellum from the rats that received monosodium L-glutamate before the weaning stage. The data from the fluorescent immunohistochemistry indicated the regulation of CYP1B1 and CYP2U1 in both neurons and glial cells following glutamate treatment. The expression levels of CYP1B1 mRNA and protein have been shown to be changed by triclosan in primary cultures of neocortical neurons from mouse embryos, indicating the regulation of CYP1B1 by exogenous compounds (Szychowski et al., 2016). The previous study has shown that CYP1B1 protein was present at a high level in the astrocytes, but not found in the neurons in human brain (Dutheil et al., 2009a). Our data showed the up-regulation of CYP1B1 proteins in both neurons (e.g. Purkinje cell) and astrocytes in rat brain. The in vitro data showed that glutamate can regulate CYP1B1 and CYP2U1 in both U251 cells and hCMEC/D3 cells. The co-localization of the CYPs and GFAP indicated the induction of astrocytic CYP1B1 and CYP2U1 by glutamate. As brain-specific CYP isoform, CYP2U1 proteins have been strongly detected in the astrocyte foot processes that contact microvessels (Dutheil et al., 2009b). The increased production of midchain and terminal HETEs by the neurotransmitter released from neurons may affect cerebral blood flow, especially under the pathological conditions.

The mGlu5 receptor, the main mGlu receptor subtype expressed in the astrocytes, has been recognized as the mediator in the cross-talk between neurons and astrocytes (Bradley and Challiss, 2012a). In the present study, we showed that the blockade of mGlu5 receptor attenuated the induction of the phosphorylated CREB proteins in the nuclear and the binding of the CREB protein with the *CYP1B1* and *CYP2U1* promoters by glutamate. Both PKA and MAPK signaling pathways triggered by mGlu5 receptor were involved in the regulation of astrocytic CYP1B1 and CYP2U1, although the regulation mechanism of CYP1B1 and CYP2U1 in hCMEC/D3 cells need to be further elucidated. It has been reported that the stimulation of mGlu5 receptors leads to robust oscillatory changes in $[Ca^{2+}]_i$, and $[Ca^{2+}]_i$ increases within astrocyte endfeet can lead to the induction of Ca^{2+}-dependent phospholipase A2 activity (Bradley and Challiss, 2012b). Our data suggest that mGlu5 receptor plays a pivotal role in the regulation of AA metabolism in the neuronal cells. As HETEs were found to play an important role in vascular homeostasis(Yousif et al., 2010; Fan and Roman, 2017), the changes in the AA metabolism may lead to vascular dysfunction. Migraine is a neurovascular disorder characterized by a decrease in cerebral blood flow and a potent dilatation of cranial extracerebral blood vessels (Maassenvandenbrink and Chan, 2008; Brennan and Andrew, 2010). Glutamate and its receptors have since long been suggested in migraine pathophysiology (Chan and MaassenVanDenBrink, 2014).A recent study suggested that mGlu5 receptor was a novel therapeutic target in the treatment of migraine in human. The blockade of mGlu5 receptor attenuated neurogenic dural vasodilation in rats, while the N-methyl-D-aspartate receptor blocker MK-801 had no effect (Waung et al., 2016). Our data support the hypothesis that the blockade of mGlu5 receptor may improve the vascular dysfunction via the alteration of the vasoactive substances from AA in the neuronal cells triggered by neurotransmitter-mediated signaling.

In conclusion, we demonstrated that extrasynaptic glutamate could in situ affect the AA metabolism via brain CYPs. CYP1B1 and CYP2U1 genes in the astrocytes are the downstream genes of CREB, and the up-regulation of CYP1B1 and CYP2U1 expression by glutamate was due to the increases in phosphorylated CREB proteins in the nuclear and the binding of the CREB protein with the *CYP1B1* and *CYP2U1* promoters. These data provided the evidence that the neuron-astrocyte reciprocal signaling can change the AA metabolism (e.g. EETs and HETEs) in astrocytes via its specific receptor. The alteration of AA deviates may affect blood flow in the microenvironment within the brain.

Conflict of interest

The authors declare no conflict of interest.

Acknowledgments

This study was supported by the Fundamental Research Funds for the Central Universities, the Program for New Century Excellent Talents in University (NCET-11-0399) and the National Natural Science Foundation of China (No. 30973582 and 81673503).

Appendix A. Supplementary data

Supplementary material related to this article can be found, in the online version, at doi:https://doi.org/10.1016/j.biocel.2019.03.001.

References

Alkayed, N.J., Birks, E.K., Hudetz, A.G., et al., 1996a. Inhibition of brain P-450 arachidonic acid epoxygenase decreases baseline cerebral blood flow. Am. J. Physiol. 271, H1541–H1546.
Alkayed, N.J., Birks, E.K., Hudetz, A.G., et al., 1996b. Inhibition of brain P-450 arachidonic acid epoxygenase decreases baseline cerebral blood flow. Am. J. Physiol. 271, H1541–H1546.
Alkayed, N.J., Narayanan, J., Gebremedhin, D., et al., 1996c. Molecular characterization of an arachidonic acid epoxygenase in rat brain astrocytes. Stroke 27, 971–979.
Amruthesh, S.C., Boerschel, M.F., McKinney, J.S., et al., 1993. Metabolism of arachidonic acid to epoxyeicosatrienoic acids, hydroxyeicosatetraenoic acids, and prostaglandins in cultured rat hippocampal astrocytes. J. Neurochem. 61, 150–159.
Attwell, D., Buchan, A.M., Charpak, S., et al., 2010. Glial and neuronal control of brain blood flow. Nature 468, 232–243.
Bradley, S.J., Challiss, R.A., 2012a. G protein-coupled receptor signalling in astrocytes in health and disease: a focus on metabotropic glutamate receptors. Biochem. Pharmacol. 84, 249–259.
Bradley, S.J., Challiss, R.A., 2012b. G protein-coupled receptor signalling in astrocytes in health and disease: a focus on metabotropic glutamate receptors. Biochem. Pharmacol. 84, 249–259.
Brennan, K.C., Andrew, C., 2010. An update on the blood vessel in migraine. Curr. Opin. Neurol. 23, 266–274.
Chan, K., MaassenVanDenBrink, A., 2014. Glutamate receptor antagonists in the management of migraine. Drugs 74, 1165–1176.
Choudhary, D., Jansson, I., Stoilov, I., et al., 2004. Metabolism of retinoids and arachidonic acid by human and mouse cytochrome P450 1b1. Drug Metab. Dispos. 32, 840–847.
Chuang, S.S., Helvig, C., Taimi, M., et al., 2004. CYP2U1, a novel human thymus- and brain-specific cytochrome P450, catalyzes omega- and (omega-1)-hydroxylation of fatty acids. J. Biol. Chem. 279, 6305–6314.
Dutheil, F., Dauchy, S., Diry, M., et al., 2009a. Xenobiotic-metabolizing enzymes and transporters in the normal human brain: regional and cellular mapping as a basis for putative roles in cerebral function. Drug Metab. Dispos. 37, 1528–1538.
Dutheil, F., Dauchy, S., Diry, M., et al., 2009b. Xenobiotic-metabolizing enzymes and transporters in the normal human brain: regional and cellular mapping as a basis for putative roles in cerebral function. Drug Metab. Dispos. 37, 1528–1538.
Dutheil, F., Jacob, A., Dauchy, S., et al., 2010. ABC transporters and cytochromes P450 in the human central nervous system: influence on brain pharmacokinetics and contribution to neurodegenerative disorders. Expert Opin. Drug Metab. Toxicol. 6, 1161–1174.
El-Sherbeni, A.A., Aboutabl, M.E., Zordoky, B.N., et al., 2013. Determination of the dominant arachidonic acid cytochrome p450 monooxygenases in rat heart, lung, kidney, and liver: protein expression and metabolite kinetics. AAPS J. 15, 112–122.
Fan, F., Roman, R.J., 2017. Effect of cytochrome P450 metabolites of arachidonic acid in nephrology. J. Am. Soc. Nephrol. Jasn. 28, 2845.
Fenghong, Z., Yingjun, L., Yaping, J., et al., 2012. Effects of arsenite on glutamate metabolism in primary cultured astrocytes. Toxicol. Vitro Int. J. Publ. Assoc. Bibra 26, 24–31.
Gebremedhin, D., Lange, A.R., Lowry, T.F., et al., 2000. Production of 20-HETE and its role in autoregulation of cerebral blood flow. Circ. Res. 87, 60–65.
Kehl, F., Cambj-Sapunar, L., Maier, K.G., et al., 2002a. 20-HETE contributes to the acute fall in cerebral blood flow after subarachnoid hemorrhage in the rat. Am. J. Physiol. Heart Circ. Physiol. 282, H1556–H1565.

Kehl, F., Cambj-Sapunar, L., Maier, K.G., et al., 2002b. 20-HETE contributes to the acute fall in cerebral blood flow after subarachnoid hemorrhage in the rat. Am. J. Physiol. Heart Circ. Physiol. 282, H1556–H1565.
Kilkenny, C., Browne, W.J., Cuthill, I.C., et al., 2010. Improving bioscience research reporting: the ARRIVE guidelines for reporting animal research. J. Pharmacol. Pharmacother. 1, 94–99.
Koehler, R.C., Roman, R.J., Harder, D.R., 2009. Astrocytes and the regulation of cerebral blood flow. Trends Neurosci. 32, 160–169.
Lewerenz, J., Maher, P., 2015. Chronic glutamate toxicity in neurodegenerative diseases-what is the evidence? Front. Neurosci. 9, 469.
Lima, C.B., Soares, G.S., Vitor, S.M., et al., 2013. Neonatal treatment with monosodium glutamate lastingly facilitates spreading depression in the rat cortex. Life Sci. 93, 388–392.
Liu, M., Zhu, Q., Wu, J., et al., 2017. Glutamate affects the production of epoxyeicosanoids within the brain: the up-regulation of brain CYP2J through the MAPK-CREB signaling pathway. Toxicology 381, 31–38.
Maassenvandenbrink, A., Chan, K.Y., 2008. Neurovascular pharmacology of migraine. Eur. J. Pharmacol. 585, 313–319.
McGrath, J.C., Drummond, G.B., McLachlan, E.M., et al., 2010. Guidelines for reporting experiments involving animals: the ARRIVE guidelines. Br. J. Pharmacol. 160, 1573–1576.
Ortuno-Sahagun, D., Gonzalez, R.M., Verdaguer, E., et al., 2014. Glutamate excitotoxicity activates the MAPK/ERK signaling pathway and induces the survival of rat hippocampal neurons in vivo. J. Mol. Neurosci. 52, 366–377.
Porter, J.T., McCarthy, K.D., 1996. Hippocampal astrocytes in situ respond to glutamate released from synaptic terminals. J. Neurosci. 16, 5073–5081.
Rose, C.F., Verkhratsky, A., Parpura, V., 2013. Astrocyte glutamine synthetase: pivotal in health and disease. Biochem. Soc. Trans. 41, 1518–1524.
Shawahna, R., Uchida, Y., Decleves, X., et al., 2011. Transcriptomic and quantitative proteomic analysis of transporters and drug metabolizing enzymes in freshly isolated human brain microvessels. Mol. Pharm. 8, 1332–1341.
Stella, N., Tence, M., Glowinski, J., et al., 1994a. Glutamate-evoked release of arachidonic acid from mouse brain astrocytes. J. Neurosci. 14, 568–575.
Stella, N., Tence, M., Glowinski, J., et al., 1994b. Glutamate-evoked release of arachidonic acid from mouse brain astrocytes. J. Neurosci. 14, 568–575.
Szychowski, K.A., Wnuk, A., Kajta, M., et al., 2016. Triclosan activates aryl hydrocarbon receptor (AhR)-dependent apoptosis and affects Cyp1a1 and Cyp1b1 expression in mouse neocortical neurons. Environ. Res. 151, 106–114.
Waung, M.W., Akerman, S., Wakefield, M., et al., 2016. Metabotropic glutamate receptor 5: a target for migraine therapy. Ann. Clin. Transl. Neurol. 3, 560–571.
Weksler, B., Romero, I.A., Couraud, P.O., 2013. The hCMEC/D3 cell line as a model of the human blood brain barrier. Fluids Barriers CNS 10, 16.
Yousif, M., Benter, I., Roman, R., 2010. Cytochrome P450 metabolites of arachidonic acid play a role in the enhanced cardiac dysfunction in diabetic rats following ischaemic reperfusion injury. Auton. Autacoid Pharmacol. 29, 33–41.
Zhu, Q.F., Hao, Y.H., Liu, M.Z., et al., 2015. Analysis of cytochrome P450 metabolites of arachidonic acid by stable isotope probe labeling coupled with ultra high-performance liquid chromatography/mass spectrometry. J. Chromatogr. A 1410, 154–163.